Available online at www.sciencedirect.com

ScienceDirect

Ceramics International 40 (2014) 181–189

CERAMICS INTERNATIONAL

www.elsevier.com/locate/ceramint

Effects of praseodymium substitution on electrical properties of $CaCu_3Ti_4O_{12}$ ceramics

Alok Kumar Rai[a], Jihyeon Gim[a], Eui-chol Shin[a], Hyun-Ho Seo[a], Vinod Mathew[a], K.D. Mandal[b], Om Parkash[c], Jong-Sook Lee[a], Jaekook Kim[a,*]

[a]Department of Materials Science and Engineering, Chonnam National University, 300 Yongbong-dong, Bukgu, Gwangju 500-757, Republic of Korea

[b]Department of Applied Chemistry, Indian Institute of Technology, Banaras Hindu University, Varanasi 221005, UP, India

[c]Department of Ceramic Engineering, Indian Institute of Technology, Banaras Hindu University, Varanasi 221005, UP, India

Received 15 May 2013; received in revised form 30 May 2013; accepted 30 May 2013
Available online 5 June 2013

Abstract

Effect of praseodymium (Pr^{3+}) substitution at Ca^{2+} site in calcium copper titanate, $CaCu_3Ti_4O_{12}$ (CCTO), has been investigated. Compositions with $x=0.10$ and 0.20 were synthesized in the system $Ca_{(1-3x/2)}Pr_xCu_3Ti_4O_{12}$ by chemical route. Crystal structure is remained cubic. X-ray diffraction and field-emission scanning electron macrographs indicate the presence of secondary phases such as $CaTiO_3$ and CuO. X-ray photoelectron spectroscopy suggests the substitution of Ca^{2+} by Pr^{3+}/Pr^{4+}. Low temperature admittance spectroscopy identified two deep trapping levels at 0.098 and 0.073 eV for $x=0.20$ and 0.078 and 0.060 eV for $x=0.10$. High temperature impedance spectroscopy shows that the grain boundary potential is 0.40 eV and 0.48 eV for $x=0.20$ and $x=0.10$ samples respectively. Pr^{3+} doping decreases dielectric loss in the bulk at low temperature but increases the dc leakage due to the lower value of grain boundary potential.

Keywords: B. Grain size; C. Electrical properties; C. Dielectric properties; D. Perovskites

1. Introduction

The perovskite titanate $CaCu_3Ti_4O_{12}$ (CCTO) is known to have a giant dielectric constant ($\sim 10^4$) which is temperature and frequency independent in a wide range of temperature [1–3]. Such a behavior makes CCTO a promising material for capacitor applications and certainly for microelectronics and microwave devices. The origin of the very high dielectric response for this non-ferroelectric material has been controversial [2–11]. Many applications of dielectric materials require low dielectric losses [12]. In CCTO, dielectric constant and dielectric loss increase proportionally, indicating that the process of energy storage is related to the mechanisms of energy dissipation (conduction process).

Comparison of the single crystal data measured using ohmic electrodes clearly indicates an internal barrier layer capacitor (IBLC) model [13,14]. According to this model, the material can be considered as an ensemble of semiconducting CCTO grains and insulating region along the grain boundaries. This IBLC model was also supported by impedance spectroscopy measurements [4,11,14–16]. Temperature and voltage dependence of the grain boundaries resistance and capacitance suggests the Schottky-type depletion layer as the origin of highly blocking grain boundary region [5,6,14–16]. The exact nature of Schottky barrier has still not been fully understood. In fact, the electronic structure of CCTO bulk crystal has not been well established. Although many reports presume the n-type conduction in CCTO due to presence of oxygen vacancies or Cu oxidation, there are also experimental evidences of p-type conduction in CCTO [17,18].

Effect of various dopants has been investigated to improve its dielectric loss characteristics by controlling the chemistry and structure of interfacial regions at grain boundaries [19–27]. Each dopant has its own preferential substitutional site when incorporated into the CCTO lattice, depending on its size and

*Corresponding author. Tel.: +82 62 530 1703; fax: +82 62 530 1699.
E-mail address: jaekook@chonnam.ac.kr (J. Kim).

0272-8842/$ - see front matter © 2013 Elsevier Ltd and Techna Group S.r.l. All rights reserved.
http://dx.doi.org/10.1016/j.ceramint.2013.05.121

valence. It has been found that some dopants have a critical influence on grain boundary barriers as well as a reduction in the number of charge carriers in the bulk grains as well [28]. Effect of dopants on the substitution stoichiometry viz. Ti deficiency [29] or excess [30] and Cu deficiency [31] or excess [32] has been also investigated.

In the present investigation, Ca^{2+} is partially substituted by Pr^{3+} ion via a modified sol–gel method with the stoichiometry $Ca_{(1-3x/2)}Pr_xCu_3Ti_4O_{12}$ ($x=0.10$, 0.20, abbreviated as CPCTO-1 and CPCTO-2 respectively) assuming the ionic compensation $[Pr_{Ca}^{\bullet}]=2[V_{Ca}'']$. Recently, Xu et al. [33] reported dielectric properties of Pr substituted CCTO ceramics prepared by solid state reaction where the compositions were determined assuming the multivalent Pr as in Pr_6O_{11}. Yet, very little fundamental insight into the effects of Pr on the defects and electronic properties of CCTO has been given. Electrical characterization was limited to the temperature range between 290 and 490 K. In the present work electrical properties were measured over a wide temperature range from 100 K to 500 K. The phase and microstructure analysis have been studied by powder X-ray diffraction (XRD) and field-emission scanning electron microscopy (FE-SEM). X-ray photoelectron spectroscopy (XPS) analysis was also carried out.

2. Experimental

Calcium acetate hydrate [$Ca(C_2H_3O_2)_2 \cdot H_2O$ 98+%, Yakuri Pure Chemicals], copper acetate monohydrate [$Cu(C_2H_3O_2)_2 \cdot H_2O$ 98+%, Sigma-Aldrich], titanium butoxide [$(C_{16}H_{36}O_4)Ti$ 97%, Sigma-Aldrich], praseodymium (III) nitrate [$Pr(NO_3)_3 \cdot 6H_2O$ 99.9%, Sigma-Aldrich] and citric acid (99.5%, Merck, India) were used as raw materials. Calculated amount of titanium butoxide was first mixed with acetic acid for 30 min with constant stirring using a magnetic stirrer. Then citric acid (equivalent to metal ions) previously dissolved in deionized water was added to the titanium solution and stirred for 30 min. A second solution consisting of measured calcium acetate, copper acetate and praseodymium nitrate was made in deionized water and added to the titanium–citric acid solution with constant stirring, resulting in a clear blue solution. A few drops of aqueous ammonia (34%) were added to the solution. The solution was heated to 80–90 °C with constant stirring to evaporate the water. During evaporation, the homogeneously mixed solution became viscous and turned into a blue gel. It was then dried in an oven at 150 °C overnight. Dried CPCTO gel was calcined in air at 800 °C for 5 h. The calcined powder was pressed into cylindrical pellets using a hydraulic press. The pressed samples were sintered at 1000 °C for 5 h in air. Heating as well as cooling rates were maintained at 5 °C/min during calcination and sintering.

Differential thermal analysis (DTA) and thermo gravimetric (TG) analysis of this as-prepared powder was performed in air atmosphere using TGA/DTA Analyzer, (TA instrument-SDT Q 600) from room temperature to 1000 °C at a heating rate of 5 °C/min. The phase composition of the samples was studied by powder X-ray diffraction analysis (Shimadzu X-ray diffractometer) with Cu Kα radiation ($\lambda=1.5406$ Å) in 2θ range 20–80°. The microstructures of the fractured surfaces were examined using a field-emission scanning electron microscope (FE-SEM, S-4700 Hitachi). Dielectric measurements were made using a pellet both surfaces of which were polished and coated with silver paint. An impedance analyzer (HP-4284A) was used to measure the impedance response in the temperature range 100–510 K controlled by a closed-cycle-refrigerator (CCR) having a high temperature option (CCS-400/202, Janis, USA).

3. Results and discussion

Fig. 1 shows the representative TG/DTA curve of the powder precursor of CPCTO-2. The figure shows that, there are three stages of weight loss: the first one is observed at the temperature ~240 °C, the second one is at ~350 °C and the third one is around 650 °C. Decomposition of citric acid and partial decomposition of precursor in the present material will lead to combustion. The first weight loss was assumed to be due to loss of residual water and decomposition of excess citric acid [34]. Corresponding changes in DTA curve are also observed as exothermic peaks in the same temperature range. The second steep decrease in weight may be due to the burnout of organic species involved in the precursor powders (organic mass remained after decomposition of citrate nitrate gel). This major weight loss in TG analysis is also supported by an intense exothermic peak in the DTA curve. The third minor weight loss in TG curve is an exothermic reaction accompanied by the decomposition of intermediate compound. No further weight loss and no thermal effect were observed above 650 °C.

Fig. 2(a and b) shows the X-ray diffraction patterns of CPCTO-1 and CPCTO-2 powders sintered at 1000 °C for 5 h respectively. The diffraction data obtained for CPCTO-1 and CPCTO-2 samples could be indexed to a body-centered cubic perovskite related structure. Copper oxide (CuO) and calcium titanate ($CaTiO_3$) are identified as impurity phases. From the peak intensity ratio, more impurity phases are shown to exist in CPCTO-2 with a higher Pr substitution. It has been shown that Ti excess can induce similar multi-phasic system [35]. The

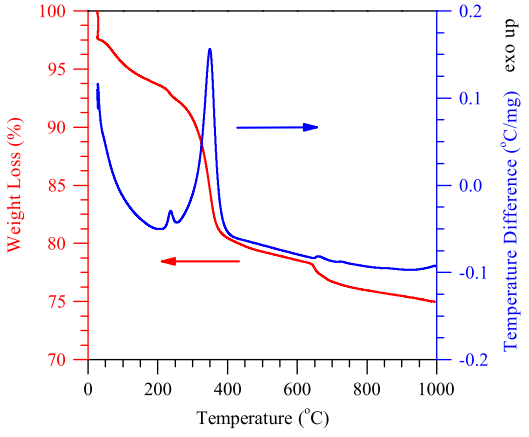

Fig. 1. Simultaneous TG—DTA curves for the precursor powder $Ca_{(1-3x/2)}Pr_xCu_3Ti_4O_{12}$ (x=0.20).

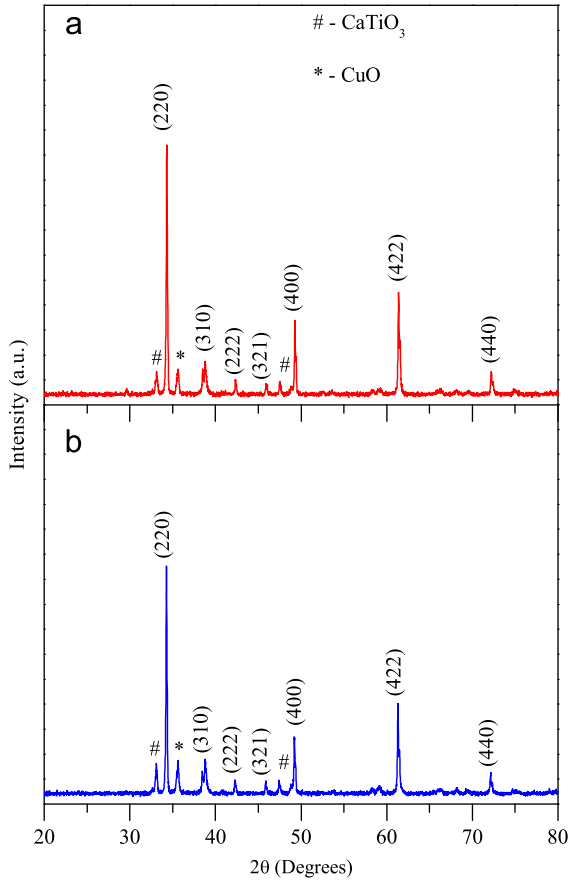

Fig. 2. X-ray powder diffraction patterns of $Ca_{(1-3x/2)}Pr_xCu_3Ti_4O_{12}$ ceramics (a) $x=0.10$ and (b) 0.20 sintered at 1000 °C for 5 h.

presence of $CaTiO_3$ may suggest a substantial Ca deficiency in CCTO crystal structure. The general observation appears consistent with the energetically favorable formation of anti-site defects Cu_{Ca} which are as high as 10^{19} cc^3 [36].

Fig. 3 shows FE-SEM images of fractured surface of CPCTO-1 and CPCTO-2 samples, respectively. The presence of the secondary phases can be clearly noted. Their distribution was rather inhomogeneous as indicated by two micrographs for each sample. Overall more secondary phases can be seen in CPCTO-2 in accordance with XRD results, Fig. 2. The grain–grain junctions by intergranular fracture can be noted. Pure CCTO also exhibits a transgranular fracture [34]. The free grain surfaces suggest the rounded or spherical CCTO grain shape when the grains do not impinge upon each other. Some parts of the microstructure suggest the crystallographic facets. The microstructure of Pr-doped CCTO is similar to that of La-doped CCTO [34]. Doping decreases the grain size. Similar doping effects on the grain size can be seen in Pr_6O_{11}–CCTO samples prepared by solid state reaction [33]. The grain boundary segregation of dopants a retarding the grain growth may be responsible for the lower grain boundary potential discussed later.

XPS analysis was carried out to investigate the oxidation states of polyvalent ions present in $Ca_{(1-3x/2)}Pr_xCu_3Ti_4O_{12}$ ($x=0.20$) ceramics. Fig. 4(a–e) shows the representative core level XPS spectra of C-1s, O-1s, Ca-2p, Pr-3d, Cu-2p and Ti-2p regions of CPCTO-2 ceramic respectively. Shift of core-level spectra due to charging effect was calibrated using the C-1s peak located at 284.6 eV as shown in Fig. 4(a). The O-1s spectrum shown in Fig. 4(b) represents a binding energy of 530.05 eV along with two or more different types of oxygen

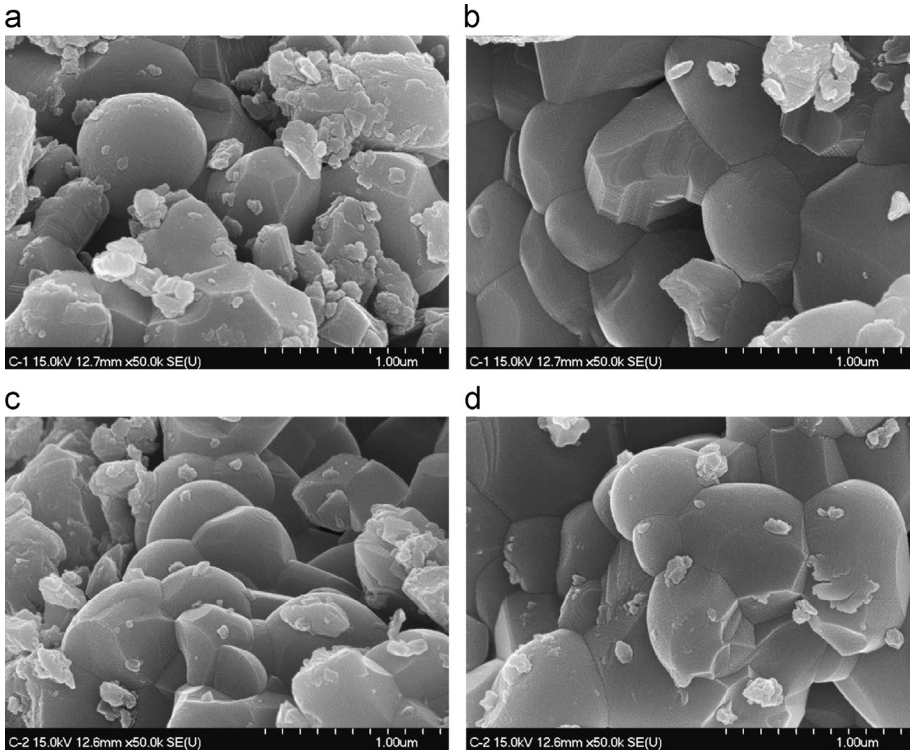

Fig. 3. FE-SEM micrographs of fractured surface of $Ca_{(1-3x/2)}Pr_xCu_3Ti_4O_{12}$ ceramics with x=0.10 (a and b) and x=0.20 (c and d).

species, which seem to be due to the substitution of Pr in Ca [37,38].

Ca-2p core-level region shows two peaks at 346.8 eV and 350.4 eV corresponding to spin–orbit doublets of Ca-$2p_{3/2}$ and Ca-$2p_{1/2}$, respectively as shown in Fig. 4(c). The spin–orbit splitting between the Ca-$2p_{3/2}$ and $2p_{1/2}$ components is about 3.6 eV. Asymmetric Ca-$2p_{3/2}$ peaks are reported in the literature for $CaTiO_3$ compounds. These were attributed to the Ca binding energy variation related to Ca superficial atoms [39]. Probably, Ca is precipitated at the grain boundary regions in CCTO ceramics and then two types of energy would be due to bulk and superficial Ca atoms. This result is also similar to that observed in $Ba_{1-x}Ca_xTiO_3$. In $Ba_{1-x}Ca_xTiO_3$ prepared by the ceramic method, some of the Ca^{2+} occupies Ti^{4+} sites in spite of a large difference in their sizes [40]. XPS analysis is similar to that observed in Fe^{3+} and Nb^{5+} doped CCTO ceramics [41] as well as undoped CCTO [42]. In CCTO ceramic, the respective shoulders on higher energy sides have been ascribed to two different occupation sites of Ca ions viz., in the CaO_{12} icosahedron and in the CuO_4 planar square [42].

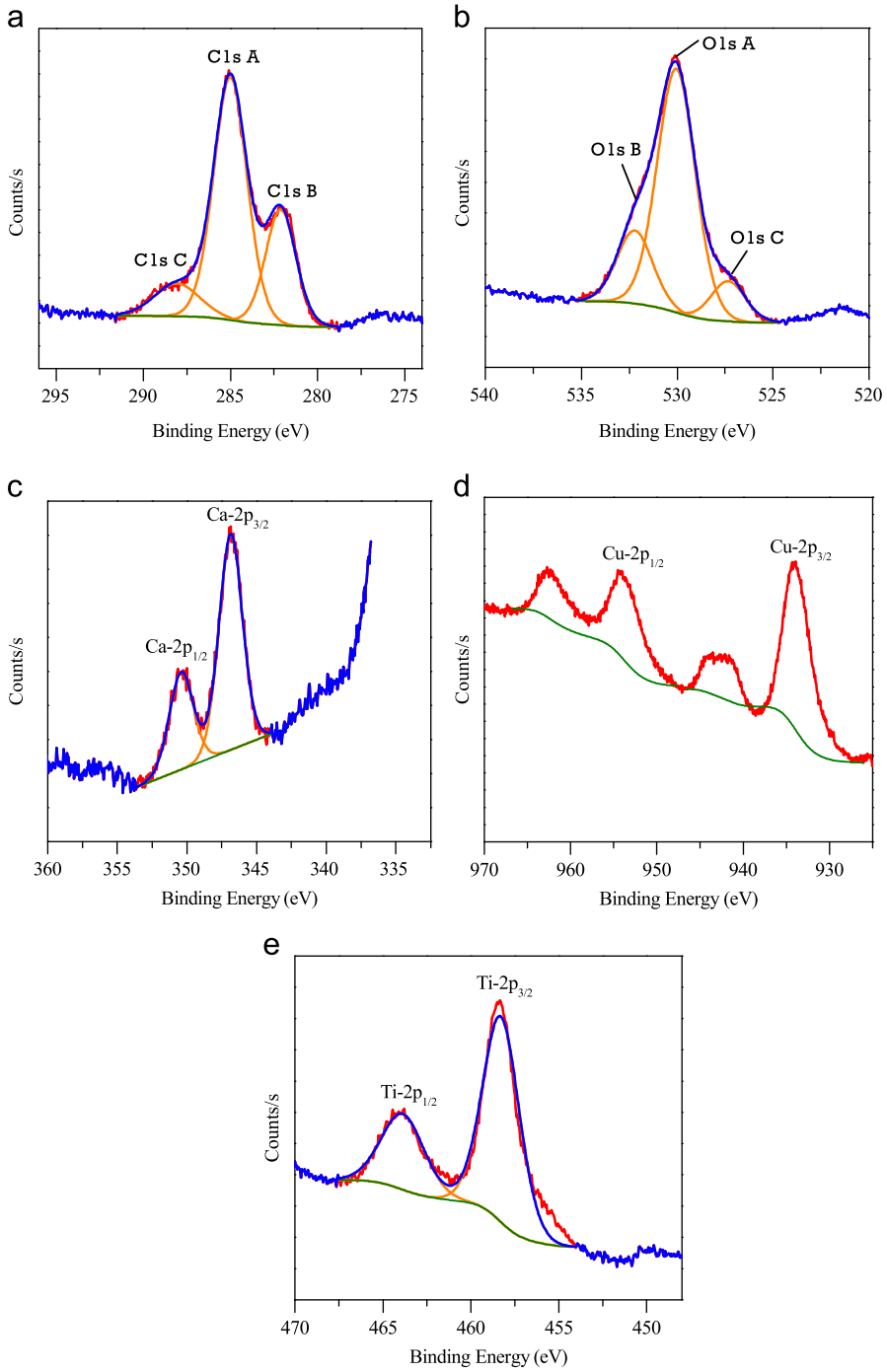

Fig. 4. X-ray photoelectron spectrum (XPS) of (a) C-1s core level, (b) O-1s core level, (c) Ca-2p core level, (d) Cu-2p core level and (e) Ti-2p core level for $Ca_{(1-3x/2)}Pr_xCu_3Ti_4O_{12}$ ($x=0.20$) ceramic.

However, the asymmetry or the presence of shoulders is not significant in CPCTO-2 ceramic of the present study, suggesting that there is no disorder present on Ca and Cu site observed in CCTO. Presence of calcium in +2 oxidation states is clear not only from the binding energy (346.8 eV) of Ca-$2p_{3/2}$ level but also from the shape and symmetry of the peak.

Fig. 4(d) displays the XPS spectra of Cu-2p region of CPCTO-2 ceramics. XPS shows Cu-$2p_{3/2}$ and Cu-$2p_{1/2}$ peaks at 934.1 eV and 954.3 eV, respectively in Fig. 4(d). Cu-$2p_{3/2}$ spectra have a satellite on the higher binding energy side which is similar to that reported for Cu^{2+} in CuO [43] or Fe^{3+} and Nb^{5+} doped CCTO ceramics [41]. The satellite peaks correspond to $2p3d^9$ configuration where 2p indicates that there is one electron missing (core hole) in the Cu-2p [30]. In a photoelectron emission process, electron charges are transferred from the surrounding to the core holes. Such a situation causes the main peak to be associated with a satellite at higher binding energy, as observed here [44]. The satellites confirm the existence of copper as Cu^{2+}. The satellite peak is absent in Cu_2O because it has a completely filled d shell (d^{10}). Since Pr peaks (Pr-$3d_{5/2}$ and the Pr-$3d_{3/2}$) overlap exactly with those of Cu [45], small amount of praseodymium doping did not allow direct information of the Pr valence state.

XPS core level spectra of Ti-2p shown in Fig. 4(e) demonstrate Ti-$2p_{3/2}$ and Ti-$2p_{1/2}$ peaks, respectively, at 458.4 eV and 463.9 eV. These are very close to the reported data for TiO_2 [46] and CCTO ceramic [47]. This shows that the Ti ions are mainly in the tetravalent state i.e. there is no change in the valence of Ti^{4+} ions when Pr^{3+} is doped on Ca site in CCTO ceramic.

Fig. 5 shows the temperature dependence of dielectric constant (ε) and dielectric loss ($\tan\delta$) of the sintered CPCTO-1 and CPCTO-2 ceramics at selected frequencies over the temperature range from 100 K to 510 K. With increasing temperature the capacitance increases from 60~63 to a plateau of 700–1000 for CPCTO-1 and 600 to 800 for CPCTO-2, respectively, followed by a rapid increase over a range of temperature. The decrease in the dielectric constants at high temperature, clearly indicated for

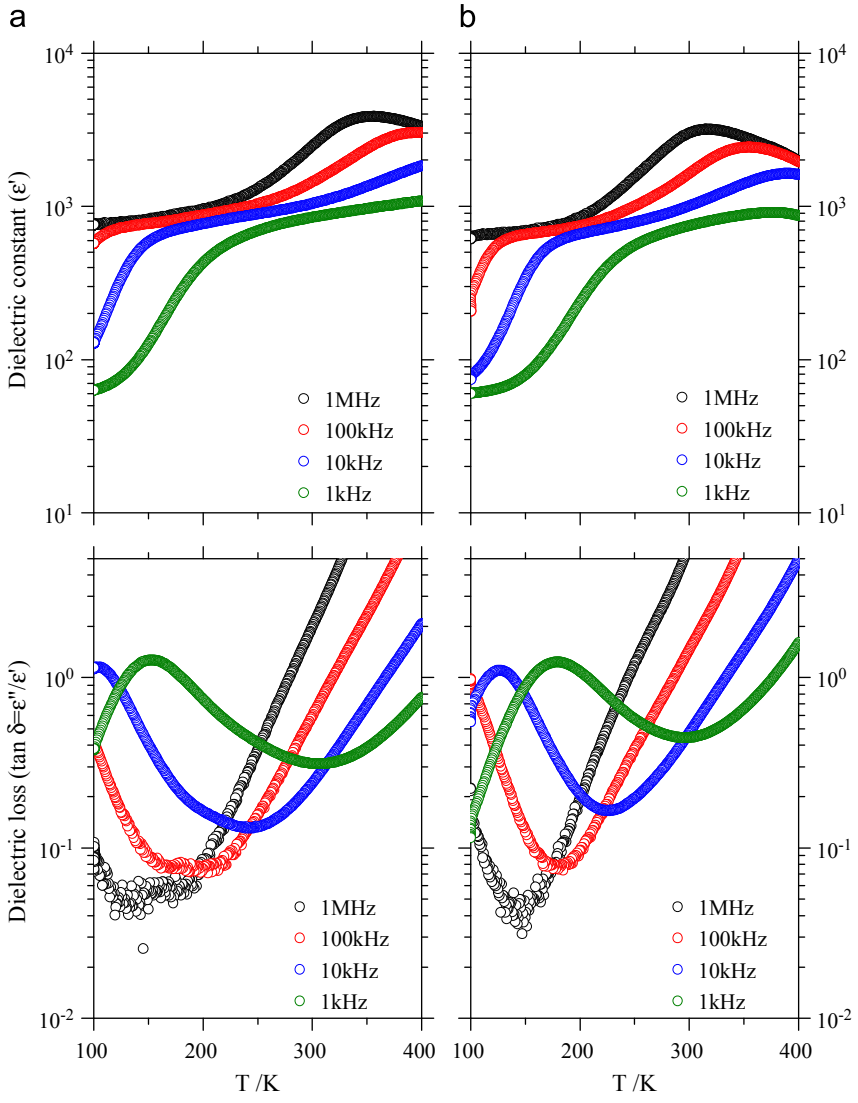

Fig. 5. The temperature dependence of dielectric constant ε (T) and dielectric loss tan δ (T) at different frequencies for $Ca_{(1-3x/2)}Pr_xCu_3Ti_4O_{12}$ ceramics with (a) $x=0.10$ and (b) 0.20.

the data at 1 kHz, is due to the inductance effects from the lead wires since the resistance of the samples becomes as small as a few ten ohms. The feature should not be mistaken as a (relaxor) ferroelectric transition.

The low temperature dielectric constants of ca. 60~63 at 1 MHz appears consistent with the optical dielectric constant reported as 80 [3] when the porosity of the samples is taken into consideration according to the effective medium approach [48].

It appears now clear [4–6,14] that the frequency-dependent capacitance rises to the sloping plateau, representing the colossal dielectric constant known for CCTO, can be attributed to the grain boundaries. Two different electrical models for the grain boundary barriers may be considered. More common is the brick-layer or layer model where the grain boundary layer is in series with the bulk response of the grains [4–6,14]. The other is the model for the admittance spectroscopy where RC series circuits representing the trapping due to the deep levels are correlated to the bulk capacitance and the resistor for the leakage current [49,50]. The latter model appears appropriate for the description of the low temperature spectra as shown in complex capacitance plane representation in Fig. 6(b and c). The ac bulk conductivity of CCTO shows a power-law or deviation from the ideal Debye behavior. Macdonald also suggests the application of anomalous Poisson–Nernst–Planck diffusion model for CCTO [51].

Although the spectra are slightly skewed at the high frequency side for $x=0.10$ and at low frequency side for $x=0.20$, respectively, the peak region appears close to the ideal Debye response. The relaxation time constants τ from the peak frequencies are displayed in Fig. 6(a). Both samples exhibit a bending or transition around −130 °C with increased activation energy by ca. 0.015 eV at higher temperature region. Above −130 °C the activation energy values are 0.075 and 0.098 eV, respectively. The values appear consistent with the reported value in pure single crystal CCTO [3,4] as well as in thin film [17]. Samples with higher Pr content exhibit larger τ values and larger activation energy. That is, the deep levels become larger due to Pr doping. The activation energy was shown to increase up to 0.15 eV by annealing the thin films in air, concomitant with the substantially decreased "colossal dielectric constants" from 2000 to 400 and reduced the dielectric losses [52]. The effect of different Pr doping as shown in Fig. 5 appears similar to the oxidation effect. Pr doping decreases the dielectric loss in the low temperature range, which may be considered beneficial for the capacitor applications. It should be mentioned however, that the low temperature response corresponds to the bulk response of CCTO in the brick-layer model of negligible portion in the insulation resistance of the polycrystalline CCTO samples as described below [4–6].

The dielectric spectra shown in Fig. 6 are asymmetric suggesting the presence of another relaxation, either at low frequency (for $x=0.10$) or at high frequency range ($x=0.20$). The low frequency effects more clearly observed for $x=0.10$ than for $x=0.20$ should be related to the larger grain boundary potential and higher insulation resistance. The dc resistance, either directly obtained from the impedance spectra as shown in Fig. 7 or extrapolated, exhibit a well-defined Arrhenius behavior of activation energies of 0.48 eV for $x=0.10$ and 0.40 eV for $x=0.20$, respectively. The values are somewhat less than reported for the pristine CCTO ceramics, e.g. 0.66 eV [6] and 0.76 eV [53]. From the present experimental results it may be concluded Pr doping decreases the insulation resistance by lowering the grain boundary or surface potential of CCTO. The lowering insulation per grain boundary may be even larger for $x=0.20$ composition, since the grain size for $x=0.20$ is smaller and thus larger number of grain boundaries may exist.

It should be noted that the effect of Pr doping on the electrical properties is opposite for the high frequency bulk effects observed in the low temperature range displayed in Fig. 6 and for high temperature dc resistance effects determined by the grain boundary potential shown in Fig. 7. Comparison of Pr doping with oxidation effects [52] on the electronic structure in the bulk and at

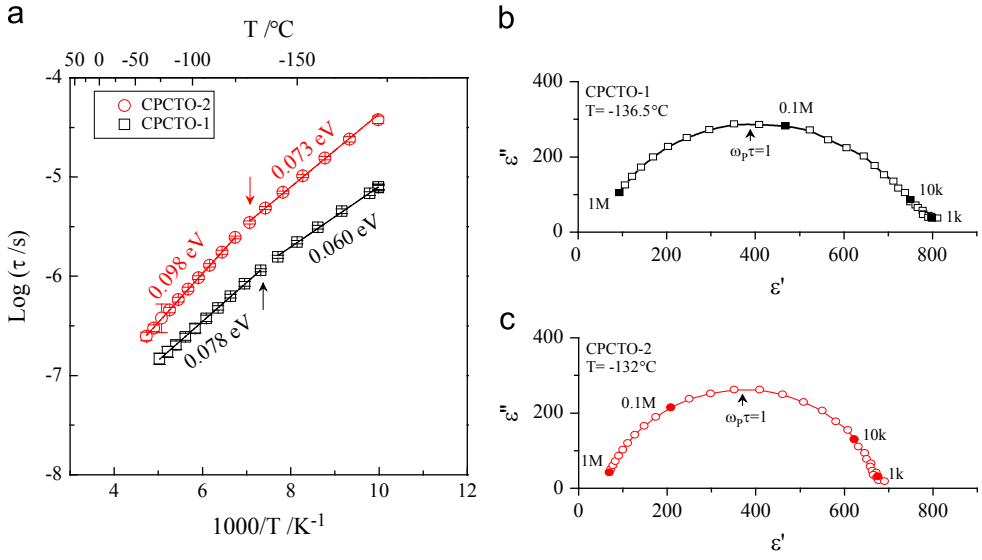

Fig. 6. The temperature dependence of dielectric relaxation time τ for $Ca_{(1-3x/2)}Pr_xCu_3Ti_4O_{12}$ ceramics with $x=0.10$ and 0.20 (a) estimated from the dielectric spectra as shown for $x=0.10$ at −136 °C (b) and for $x=0.20$ at −132 °C (c) which is indicated by arrows in (a).

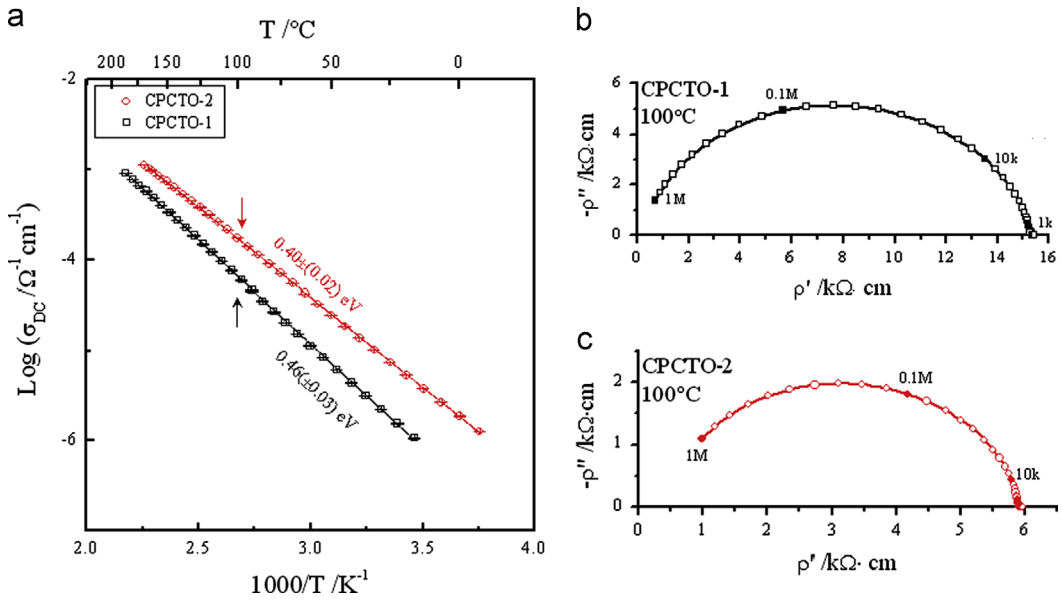

Fig. 7. The temperature dependence of dc conductivity for $Ca_{(1-3x/2)}Pr_xCu_3Ti_4O_{12}$ ceramics with $x=0.10$ and 0.20 (a) estimated from the impedance spectra as shown for $x=0.10$ (b) and for $x=0.20$ (c) at 100 °C which is indicated by arrows in (a).

the grain boundary suggests the p-type conduction of CCTO [17,18] although no clear mechanism of p-type conduction in CCTO has been yet established. It may be suggested that the abundant anti-site defects Cu_{Ca} may act as acceptor 'Cu'_{Ca} in Cu^{+} state. Pr substituting Ca ions may thus affect the characteristics of trapping acceptor levels. Assuming CCTO a p-type conductor, the grain boundary potential can be lowered by the grain boundary segregation of the negatively charged defects or acceptors, opposite to the well-known n-type conductors, such as $BaTiO_3$ PTCR and ZnO varistors. The segregated praseodymium in n-type ZnO is one of the representative varistor-forming dopant [50]. Note that the effects of the oxidation and sintering atmosphere in the grain boundary or electrode Schottky barriers in CCTO in the literature seems not yet unambiguously indicating the conduction type of CCTO [11,17,18,54,55]. It is highly likely that secondary phases, segregation, and multiple electronic states of Cu and Ti depending on the preparation and post-treatments are taken into play together. The exact nature of the defects responsible for the electrical properties of the bulk and grain boundaries in CCTO needs further clarification. Strong disagreement between the present work and Pr-doped CCTO [33] in the microstructural evolution and the electrical properties is also suggested to the difference in the initial stoichiometry with Pr dopant, i.e. Pr_2O_3 vs. Pr_6O_{11}, which in addition to the preparative routes should affect the electronic structure of bulk and grain boundaries.

4. Conclusions

In summary, Pr doped CCTO ceramics such as $Ca_{(1-3x/2)}Pr_xCu_3Ti_4O_{12}$ (CPCTO) ($x=0.10$ and 0.20) were synthesized by chemical route. XRD analysis confirmed the major phase formation of CCTO in the prepared CPCTO samples with the presence of CuO and $CaTiO_3$ secondary phases at 1000°C/5 h. FE-SEM image shows faceted morphology and spherical appearance for grains having sizes in the range of 300–800 nm for both CPCTO samples. The low temperature dielectric relaxation indicated the trapping levels are higher for $x=0.20$ than for $x=0.10$ samples: 0.073 and 0.060 eV, respectively, below −130 °C and 0.098 and 0.078 eV, respectively below −50 °C, leading to the low loss for the sample with higher Pr doping. From the high temperature dc behavior, the grain boundary Schottky barrier was found lower for $x=0.20$ than for $x=0.10$, i.e. 0.48 eV and 0.40 eV, respectively, with correspondingly decreased dc insulation resistance. Pr doping apparently plays the opposite effects on the loss mechanism of bulk and grain boundary. A p-type conduction mechanism for CCTO is suggested for the observed electrical behavior.

Acknowledgment

This research was supported by World Class University (WCU) program through the Korea Science and Engineering Foundation funded by the Ministry of Education, Science and Technology (R32-20074). This work was also supported by Priority Research Centers Program through the National Research Foundation of Korea (NRF) funded by the Ministry of Education, Science and Technology (2009-0094055).

References

[1] M.A. Subramanian, D. Li, N. Duan, B.A. Reisner, A.W. Sleight, High dielectric constant in $ACu_3Ti_4O_{12}$ and $ACu_3Ti_3FeO_{12}$ phases, Journal of Solid State Chemistry 151 (2000) 323–325.
[2] A.P. Ramirez, M.A. Subramanian, M. Gardel, G. Blumberg, D. Li, T. Vogt, S.M. Shapiro, Giant dielectric response in a copper-titanate, Solid State Communication 115 (2000) 217–220.
[3] C.C. Homes, T. Vogt, S.M. Shapiro, S. Wakimoto, A.P. Ramirez, Optical response of high-dielectric-constant perovskite-related oxide, Science 293 (2001) 673–676.

[4] D.C. Sinclair, T.B. Adams, F.D. Morrison, A.R. West, $CaCu_3Ti_4O_{12}$: one-step internal barrier layer capacitor, Applied Physics Letters 80 (2002) 2153.
[5] T.B. Adams, D.C. Sinclair, A.R. West, Giant barrier layer capacitance effects in $CaCu_3Ti_4O_{12}$ ceramics, Advanced Materials 14 (2002) 1321–1323.
[6] T. Adams, D. Sinclair, A. West, Characterization of grain boundary impedances in fine- and coarse-grained $CaCu_3Ti_4O_{12}$ ceramics, Physical Review B 73 (2006) 094124.
[7] P. Lunkenheimer, V. Bobnar, A.V. Pronin, A.I. Ritus, A.A. Volkov, A. Loidl, Origin of apparent colossal dielectric constants, Physical Review B 66 (2002) 052105.
[8] M.H. Cohen, J.B. Neaton, L. He, D. Vanderbilt, Extrinsic models for the dielectric response of $CaCu_3Ti_4O_{12}$, Journal of Applied Physics 94 (2003) 3299–3306.
[9] P. Lunkenheimer, R. Fichtl, S.G. Ebbinghaus, A. Loidl, Nonintrinsic origin of the colossal dielectric constants in $CaCu_3Ti_4O_{12}$, Physical Review B 70 (2004) 172102.
[10] J. Yang, M. Shen, L. Fang, The electrode/sample contact effects on the dielectric properties of the $CaCu_3Ti_4O_{12}$ ceramic, Materials Letters 59 (2005) 3990–3993.
[11] J. Li, A.W. Sleight, M.A. Subramanian, Evidence for internal resistive barriers in a crystal of the giant dielectric constant material: $CaCu_3Ti_4O_{12}$, Solid State Communication 135 (2005) 260–262.
[12] W.C. Ribeiro, R.G.C. Araújo, P.R. Bueno, The dielectric suppress and the control of semiconductor non-Ohmic feature of $CaCu_3Ti_4O_{12}$ by means of tin doping, Applied Physics Letters 98 (2011) 132906.
[13] M.J. Pan, B.A. Bender, A bimodal grain size model for predicting the dielectric constant of calcium copper titanate ceramics, Journal of American Ceramic Society 88 (2005) 2611–2614.
[14] M.C. Ferrarelli, D.C. Sinclair, A.R. West, H.A. Dabkowsk, A. Dabkowski, G.M. Luke, Comment on the origin(s) of the giant permittivity effect in $CaCu_3Ti_4O_{12}$ single crystals and ceramics, Journal of Materials Chemistry 19 (2009) 5916–5919.
[15] M. Li, A. Feteira, D.C. Sinclair, A.R. West, Influence of Mn doping on the semiconducting properties of $CaCu_3Ti_4O_{12}$ ceramics, Applied Physics Letters 88 (2006) 232903.
[16] S.Y. Chung, I.L.D. Kim, S.J.L. Kang, Strong nonlinear current–voltage behaviour in perovskite-derivative calcium copper titanate, Nature Materials 3 (2004) 774–778.
[17] G. Deng, Z. He, P. Muralt, Physical aspects of colossal dielectric constant material $CaCu_3Ti_4O_{12}$ thin films, Journal of Applied Physics 105 (2009) 084106.
[18] E. Joanni, R. Savu, P. Bueno, E. Longo, J. Varela, P-type semiconducting gas sensing behavior of nanoporous rf sputtered $CaCu_3Ti_4O_{12}$ thin films, Applied Physics Letters 92 (2008) 132110.
[19] G.F. Vander Voort, A.M. Gokhale, Comments on grain size measurements using the point-sampled intercept technique, Scripta Materialia 26 (1992) 1655–1660.
[20] R.D. Shannon, C.T. Prewitt, Revised values of effective ionic radii, Acta Crystallographica B 26 (1970) 1046–1048.
[21] C.H. Mu, P. Liu, Y. He, J.P. Zhou, H. Wu, Zhang, An effective method to decrease dielectric loss of $CaCu_3Ti_4O_{12}$ ceramics, Journal of Alloys and Compounds 471 (2009) 137–141.
[22] S.Y. Chung, S.I. Lee, J.H. Choi, S.Y. Choi, Initial cation stoichiometry and current–voltage behavior in Sc-doped calcium copper titanate, Applied Physics Letters 89 (2006) 191907.
[23] S.F. Shao, J.L. Zhang, P. Zheng, C.L. Wang, J.C. Li, M.L. Zhao, High permittivity and low dielectric loss in ceramics with the nominal compositions of $CaCu_{3-x}La_{2x/3}Ti_4O_{12}$, Applied Physics Letters 91 (2007) 042905.
[24] E.A. Patterson, S. Kwon, C.C. Huang, D.P. Cann, Effects of ZrO_2 additions on the dielectric properties of $CaCu_3Ti_4O_{12}$, Applied Physics Letters 87 (2005) 182911.
[25] Y. Yan, L. Jin, L. Feng, G. Cao, Decrease of dielectric loss in giant dielectric constant $CaCu_3Ti_4O_{12}$ ceramics by adding $CaTiO_3$, Materials Science and Engineering B 130 (2006) 146–150.
[26] S. Kwon, C.C. Huang, E.A. Patterson, D.P. Cann, E.F. Alberta, S. Kwon, The effect of Cr_2O_3, Nb_2O_5 and ZrO_2 doping on the dielectric properties of $CaCu_3Ti_4O_{12}$, Materials Letters 62 (2008) 633–636.
[27] W. Kobayashi, I. Terasaki, $CaCu_3Ti_4O_{12}/CaTiO_3$ composite dielectrics: Ba/Pb-free dielectric ceramics with high dielectric constants, Applied Physics Letters 87 (2005) 032902.
[28] H.T. Yu, H.X. Liu, H. Hao, D.B. Luo, M.H. Cao, Dielectric properties of $CaCu_3Ti_4O_{12}$ ceramics modified by $SrTiO_3$, Materials Letters 62 (2008) 1353–1355.
[29] K. Chen, Y.F. Liu, F. Gao, Z.L. Du, J.M. Liu, X.N. Ying, Ti deficiency effect on the dielectric response of $CaCu_3Ti_4O_{12}$ ceramics, Solid State Communications 141 (2007) 440–444.
[30] Y.H. Lin, J. Cai, M. Li, C.W. Nan, High dielectric and nonlinear electrical behaviors in TiO_2-rich $CaCu_3Ti_4O_{12}$ ceramics, Applied Physics Letters 88 (2006) 172902.
[31] T.T. Fang, L.T. Mei, Evidence of Cu deficiency: a key point for the understanding of the mystery of the giant dielectric constant in $CaCu_3Ti_4O_{12}$, Journal of American Ceramic Society 90 (2007) 638–640.
[32] B.S. Prakash, K.B.R. Varma, The influence of the segregation of Cu-rich phase on the microstructural and impedance characteristics of $CaCu_3Ti_4O_{12}$ ceramics, Journal of Materials Science 42 (2007) 7467–7477.
[33] L.F. Xu, P.B. Qi, X.P. Song, X.J. Luo, C.P. Yang, Dielectric relaxation behaviors of pure and Pr_6O_{11}-doped $CaCu_3Ti_4O_{12}$ ceramics in high temperature range, Journal of Alloys and Compounds 509 (2011) 7697–7701.
[34] A.K. Rai, K.D. Mandal, D. Kumar, O. Parkash, Dielectric properties of lanthanum-doped $CaCu_3Ti_4O_{12}$ synthesized by semi-wet route, Journal of Physics and Chemistry of Solids 70 (2009) 834–839.
[35] S. Guillemet-Fritsch, T. Lebey, M. Boulos, B. Durand, Dielectric properties of $CaCu_3Ti_4O_{12}$ based multiphased ceramics, Journal of the European Ceramic Society 26 (2006) 1245–1257.
[36] P. Delugas, P. Alippi, V. Raineri, Native point defects in $CaCu_3Ti_4O_{12}$, IOP Conference Series: Materials Science and Engineering 8 (2010) 012015.
[37] A.V. Arakcheeva, D. Yu., V.M. Pushcharovskii, V.A. Gekimyants, G. U. Popov, Lubman, crystal structure and microtwinning of natural orthorhombic perovskite $CaTiO_3$, Crystallography Reports 42 (1997) 46–54.
[38] X. Deng, A. Verdaguer, T. Herranz, C. Weis, H. Bluhm, M. Salmeron, Surface chemistry of Cu in the presence of CO_2 and H_2O, Langmuir 24 (2008) 9474–9478.
[39] P.R. Bueno, R. Tararan, R. Parra, E. Joanni, M.A. Ramirez, W. C. Ribeiro, E. Longo, J.A. Varela, A polaronic stacking fault defect model for $CaCu_3Ti_4O_{12}$ material: an approach for the origin of the huge dielectric constant and semiconducting coexistent features, Journal of Physics D: Applied Physics 42 (2009) 055404.
[40] P.S.R. Krishna, D. Pandey, V.S. Tiwari, R. Chakravarthy, B. A. Dasannacharya, Effect of powder synthesis procedure on calcium site occupancies in barium calcium titanate: a Rietveld analysis, Applied Physics Letters 62 (1993) 231–233.
[41] J.F. Fernandez, P. Leret, J.J. Romero, J.D. Frutos, M.A. de la Rubia, M. S. Martin Gonzalez, J.L. Costa Kramer, J.L. Garcia Fierro, A. Quesada, M.A. Garcia, Proofs of the coexistence of two magnetic contributions in pure and doped $CaCu_3Ti_4O_{12}$ giant dielectric constant ceramics, Journal of American Ceramic Society 92 (2009) 2311–2318.
[42] Z.H. Sun, C.H. Kim, H.B. Moon, Y.H. Jang, J.H. Cho, C.H. Song, Y. S. Yang, Effect of Mn doping on the electronic structures of $CaCu_3Ti_4O_{12}$ ceramics, Journal of Korean Physical Society 54 (2009) 881–885.
[43] J. Ghijsen, L.H. Tjeng, J. Van Elp, H. Eskes, J. Westerink, G. A. Sawatzky, Electronic structure of Cu_2O and CuO, Physical Review B 38 (1988) 11322–11330.
[44] S. Sarkar, P.K. Jana, B.K. Chaudhuri, Copper (II) oxide as a giant dielectric material, Applied Physics Letters 89 (2006) 212905.
[45] A. Durán, E. Martínez, J.A. Díaz, J.M. Siqueiros, Ferroelectricity at room temperature in Pr-doped $SrTiO_3$, Journal of Applied Physics 97 (2005) 104109.
[46] R. Zimmermann, P. Steiner, R. Claessen, F. Reinert, S. Hufner, Electronic structure systematics of 3d transition metal oxides, Journal of Electron Spectroscopy and Related Phenomena 96 (1998) 179–186.
[47] S. Sarkar, B.K. Chaudhuri, H.D. Yang, Nanostripe domains in $CaCu_3Ti_4O_{12}$: its origin and influences on high permittivity response, Journal of Applied Physics 108 (2010) 014114.

[48] D.A.G. Bruggeman, Berechnung verschiedener physikalischer Konstanten vor heterogenen Substanzen, Annalen der Physik (Leipzig) 24 (1935) 636–664.
[49] D.L. Losee, Admittance spectroscopy of impurity levels in Schottky barriers, Journal of Applied Physics 46 (1975) 2204–2214.
[50] J.S. Lee, Y. Kim, E.C. Shin, J. Maier, Positive temperature coefficient resistor behavior in praseodymium-doped ZnO $(000\bar{1})|(000\bar{1})$ boundaries, Applied Physics Letters 96 (2010) 202104.
[51] J. Macdonald, L. Evangelista, E. Lenzi, G. Barbero, Comparison of impedance spectroscopy expressions and responses of alternate anomalous Poisson–Nernst–Planck diffusion equations for finite-length situations, Journal of Physical Chemistry C 115 (2011) 7648–7655.
[52] G. Deng, P. Muralt, Annealing effects on electrical properties and defects of $CaCu_3Ti_4O_{12}$ thin films deposited by pulsed laser deposition, Physical Review B 81 (2010) 224111.
[53] L. Ni, X.M. Chen, X.Q. Liu, Structure and modified giant dielectric response in $CaCu_3(Ti_{1-x}Sn_x)_4O_{12}$ ceramics, Materials Chemistry and Physics 124 (2010) 982–986.
[54] P. Leret, M. De La Rubia, J. Romero, J. Fernandez, Relevance of the percentage of active barriers in the dielectric response of $CaCu_3Ti_4O_{12}$ ceramics, Journal of American Ceramic Society 93 (2010) 1866–1868.
[55] L. Mei, H. Hsiang, T. Fang, Effect of copper-rich secondary phase at the grain boundaries on the varistor properties of $CaCu_3Ti_4O_{12}$ ceramics, Journal of American Ceramic Society 91 (2008) 3735–3737.